Numerical Simulation Of Epidemic Prevention And Ventilation Efficiency In Indoor Spaces With Partitions And An Air Curtain

Kun-Liang Hsieh[1], Yu-Hsuan Lee[2*], Che-Yin Lee[3], Shu-Yu Peng[1], and Shi-Min Lee[2]

[1] *Department of Mechanical and Electro-Mechanical Engineering, Tamkang University, New Taipei City, Taiwan, R.O.C.*
[2] *Department of Aerospace Engineering, Tamkang University, New Taipei City, Taiwan, R.O.C.*
[3] *Department of Refrigeration and Air Conditioning and Energy Engineering, National Chin-Yi University of Technology, Taichung City, Taiwan, R.O.C.*
[*] *Corresponding author. E-mail: hfyuhsuan98@outlook.com*

Received: May 06, 2023; Accepted: Aug. 04, 2023

In this study, computational fluid dynamics (CFD) were used to simulate the effect of a partition and air curtain on the concentration of a pollution source in an indoor space with different ventilation configurations. First, in the partition simulation, the performances of six different ventilation configurations were compared. Based on the results obtained, air curtain simulations were then carried out. In this study, carbon dioxide was chosen as the tracer gas in all simulations, and the realizable $k-\varepsilon$ turbulence model was selected. In the partition simulation, a front-and-back ventilation configuration with ventilation inlets/outlets near the side walls (in diagonal) showed the best performance. This configuration was adopted for the air curtain simulation so as to investigate the effect of different air inlet velocities and air curtain velocities. It was found that as the height of the partition increases, although it has a higher chance of blocking the Covid-19 virus, it lowers the ventilation efficiency, resulting in the increase of carbon dioxide concentration in the indoor space. When the partition was replaced with an air curtain, it was found that the higher the height of the air curtain, the lower the carbon dioxide concentration in the indoor space. Compared with the partition, the air curtain can reduce the carbon dioxide concentration by up to 74.6%, indicating that the introduction of the air curtain can have an improving effect on the ventilation in the indoor space.

Keywords: COVID-19, Air Curtain, Ventilation, Partition, CFD, Two-fluid Model

http://dx.doi.org/10.6180/jase.202405_27(5).0005

1. Introduction

In December 2019, a novel coronavirus (SARS-CoV-2) emerged from Wuhan, China, and resulted in a worldwide pandemic. The disease is officially named the Coronavirus Disease2019 (COVID-19). According to current evidence, the COVID-19 virus is primarily transmitted between people through respiratory droplets and contact vector routes. Due to the rapid spread of the virus, it has attracted global attention [1, 2].

Therefore, to prevent the spread of the virus, one must wear a mask as long as they are in an indoor environment (such as classrooms, public transportation, supermarkets, etc.). In addition to wearing masks, we also need to implement social distancing, meaning to keep a safe distance from others [3, 4] or use partitions if necessary. The so-called safety distance is 1 meter according to the norms of the WHO, which is determined based on the shedding of respiratory droplets (aerosolized via sneezing or coughing) [5].

Some studies have pointed out that the partitions used in restaurants, offices, etc. may be ineffective in preventing the spread of the COVID-19 virus, and hinder normal air flow, creating a "dead zone" where the virus accumulates.

Wang et al. [6] also suggested that the main transmission route of the virus is via aerosol transmission, implying that the virus particles will float and stay in the air. Moreover, aerosol can spread farther than the standard social distance measurement adopted by most people. This evidence shows that the partitions are ineffective in blocking the virus [7].

2. Research methodology

2.1. Governong equations

FLUENT uses the Navier-Stokes equation to solve the conservation of mass, momentum and energy equations in fluid mechanics. When the fluid has a Mach number lower than 0.3, it will be regarded as an incompressible fluid; therefore, the compressible term can be ignored. According to the characteristics of the abovementioned fluid, its governing equations are briefly described as follows: Continuity Equation:

$$\nabla \cdot (\rho \vec{v}) = 0 \tag{1}$$

Momentum Conservation Equation:

$$\frac{\partial}{\partial t}(\rho \vec{v}) + \nabla \cdot (\rho \vec{v}\vec{v}) = -\nabla p + \rho \overrightarrow{g} + \overrightarrow{F} \tag{2}$$

Energy Conservation Equation:

$$\frac{\partial}{\partial t}(\rho \mathrm{E}) + \nabla \cdot (\vec{v}(\rho \mathrm{E} + \mathrm{p})) = -\nabla \cdot \left(\sum_{\mathrm{j}} \mathrm{h_j J_j}\right) + \mathrm{S_h} \tag{3}$$

In the equations above:

P : is the pressure of the fluid ρ : is the density of the fluid ; $\rho \overrightarrow{g}$ is the gravitational force ; $\overrightarrow{F}$: is the external force including the user-defined sources ; h_j : is the enthalpy; $\mathrm{J_j}$: is the diffusion flux; $\mathrm{S_h}$: is the heat source, this term can be different external heat sources, such as chemical reaction, etc.

2.2. k- ε turbulence model equation

The $\mathrm{k} - \varepsilon$ turbulence model is a typical two-equation turbulence model, which consists of the turbulent kinetic energy equation (k) and the turbulent dissipation rate equation (ε). The $\mathrm{k} - \varepsilon$ turbulence model is further divided into three categories: standard, RNG, and realizable. The realizable k- ε turbulence model was used in this study.

Turbulent kinetic energy equation (k) :

$$\frac{\partial}{\partial t}(\rho k) + \frac{\partial}{\partial x_j}\left(\rho k u_j\right) = \frac{\partial}{\partial x_j}\left[\left(\mu + \frac{\mu_t}{\sigma_k}\right)\frac{\partial k}{\partial x_j}\right] + P_k + P_b - \rho\varepsilon - Y_M + S_k \tag{4}$$

Turbulent dissipation rate equation (ε) :

$$\frac{\partial}{\partial t}(\rho \varepsilon) + \frac{\partial}{\partial x_j}\left(\rho \varepsilon u_j\right) = \frac{\partial}{\partial x_j}\left[\left(\mu + \frac{\mu_t}{\sigma_\varepsilon}\right)\frac{\partial \varepsilon}{\partial x_j}\right] + \rho C_1 S\varepsilon - \rho C_2 \frac{\varepsilon^2}{k + \sqrt{v\varepsilon}} + C_{1\varepsilon}\frac{\varepsilon}{k}C_{3\varepsilon}G_b + S_\varepsilon \tag{5}$$

There are some adjustable constants in these two equations. After several iterations, the more widely used values were found, as follows: $C_{1\varepsilon} = 1.44, C_{2\varepsilon} = 1.92, \sigma_k = 1.0, \sigma_\varepsilon = 1.3$

2.3. Mass transfer equation

When deciding to solve a conservation equation for chemical substances, ANSYS FLUENT predicts the local mass fraction for each substance by solving the convection diffusion equation for the ith substance Y_i.

Mass transfer equation is:

$$\frac{\partial}{\partial t}(\rho Y_i) + \nabla \cdot (\rho \vec{v} Y_i) = -\nabla \cdot \vec{J}_i + R_i + S_i \tag{6}$$

In the equation above:

R_i : is the net rate of formation of substance i through a chemical reaction ;

S_i : is the creation rate added for the dispersed phase and any user-defined sources.

3. Model establishment and boundary setting

3.1. Physical model

In this study, the indoor space adopted the horizontal ventilation method: left-and-right and front-and-back configuration as shown in Fig. 1(a) and Fig. 1(b), respectively. The shape of the interior space was a cuboid, and its dimensions were $6 \times 6 \times 3$ (unit: m). The dimensions of the table were $2 \times 1.5 \times 0.7$ (unit: m), and the dimensions of the chair were $1.8 \times 0.3 \times 0.45$ (unit: m). The height of the breathing zone of the human body was 1.2 m from the ground, and the dimensions were 6×3 (unit: cm). The dimensions of the ventilation inlet/outlet were 1×0.5 (unit: m). The height from human body mouth to the table was 60 (unit: cm).The height of the partition and the air curtain was 50 cm and 100 cm, respectively and the dimensions of the base of the air column were 50×50 (unit: cm) as shown in Fig. 2.

Ventilation configuration 1: The left-and-right ventilation configuration was adopted; the air inlet was placed on the right wall, while the air outlet was placed on the left wall. The center position of the ventilation inlet/outlet was set at the midpoint horizontally, and 2.2 m above the ground as shown in Fig. 3(a).

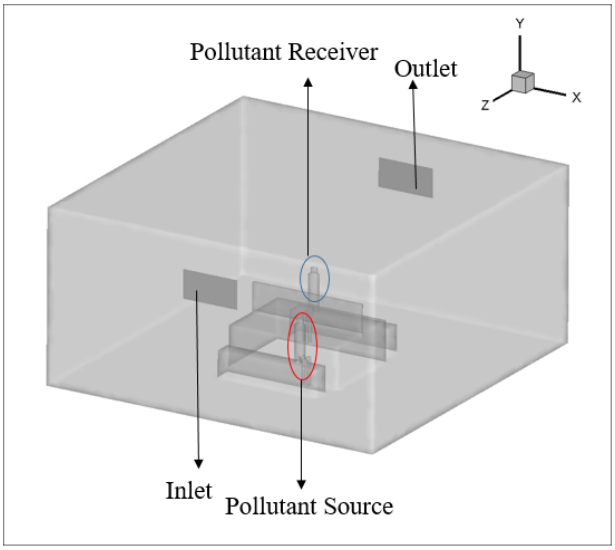

(a)

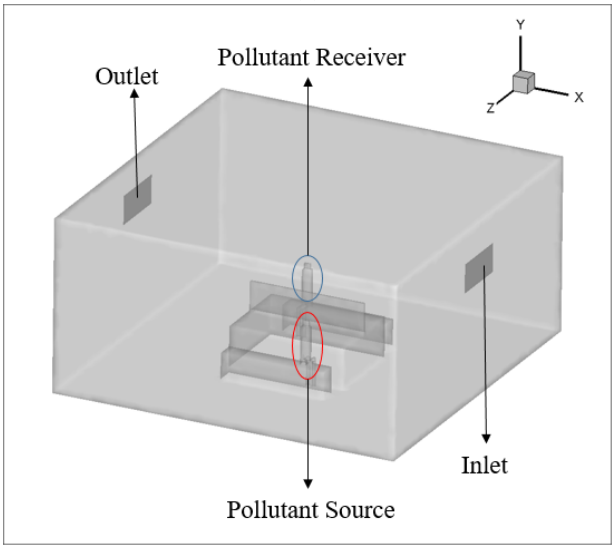

(b)

Fig. 1. (a) Physical model of left-and-right horizontal ventilation configuration. (b) Physical model of front-and-back horizontal ventilation configuration

Ventilation configuration 2: Same as ventilation configuration 1, the left-and-right ventilation configuration was adopted; the air inlet was placed on the right wall, while the air outlet was placed on the left wall. The center position of the ventilation inlet/outlet was 0.8 m away from the side wall horizontally, and 2.2 m above the ground as shown in Figure Fig. 3(b).

Ventilation configuration 3: The front-and-back ventilation configuration was adopted, and the air inlet was placed on the back wall, while the air outlet was placed on the front wall. The center position of the ventilation inlet/outlet was set at the midpoint horizontally, and 2.2 m above the ground as shown in Fig. 3(c).

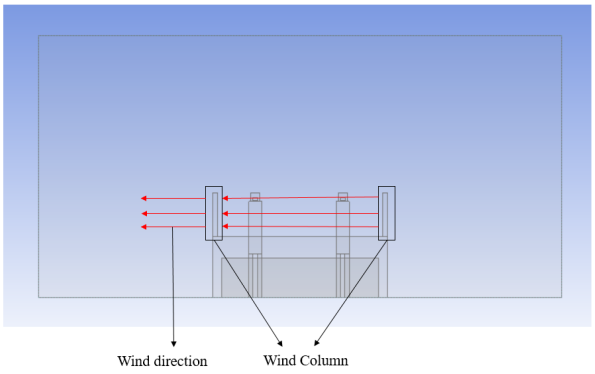

Fig. 2. Front view of the physical model of an air curtain

Ventilation configuration 4: Same as ventilation configuration 3, the front-and-back ventilation configuration was adopted; the air inlet was placed on the back wall, while the air outlet was placed on the front wall. The center position of the ventilation inlet/outlet was 0.8 m away from the side wall horizontally, and 2.2 m above the ground as shown in Fig. 3(d) and Fig. 4(a).

Ventilation configuration 5: Same as ventilation configuration 2, the left-and-right ventilation configuration was adopted; the air inlet was placed on the right wall, while the air outlet was placed on the left wall. The center position of the ventilation inlet/outlet was 0.8 m away from the side wall horizontally. The center position of the ventilation outlet was 2.2 m above the ground, while that of the ventilation inlet was 0.8 m above the ground as shown in Fig. 3(e) and Fig. 4(b).

Ventilation configuration 6: Same as ventilation configuration 4, the front-and-back ventilation configuration was adopted; the air inlet was placed on the back wall, while the air outlet was placed on the front wall. The center position of the ventilation inlet/outlet was 0.8 m away from the side wall horizontally. The center position of the ventilation outlet was 2.2 m above the ground, while that of the ventilation inlet was 0.8 m above the ground as shown in Fig. 3(f).

3.2. Basic assumptions and boundary conditions

After establishing the grid of the three-dimensional indoor space, a commercial software, FLUENT, was used to proceed with the solution setting, which includes dividing the model into three parts: fluid, partition, and human body, configuring the air inlet/outlet position, and setting the required parameters and boundary conditions.

In this study, numerical simulation analysis was carried out based on the following assumptions:

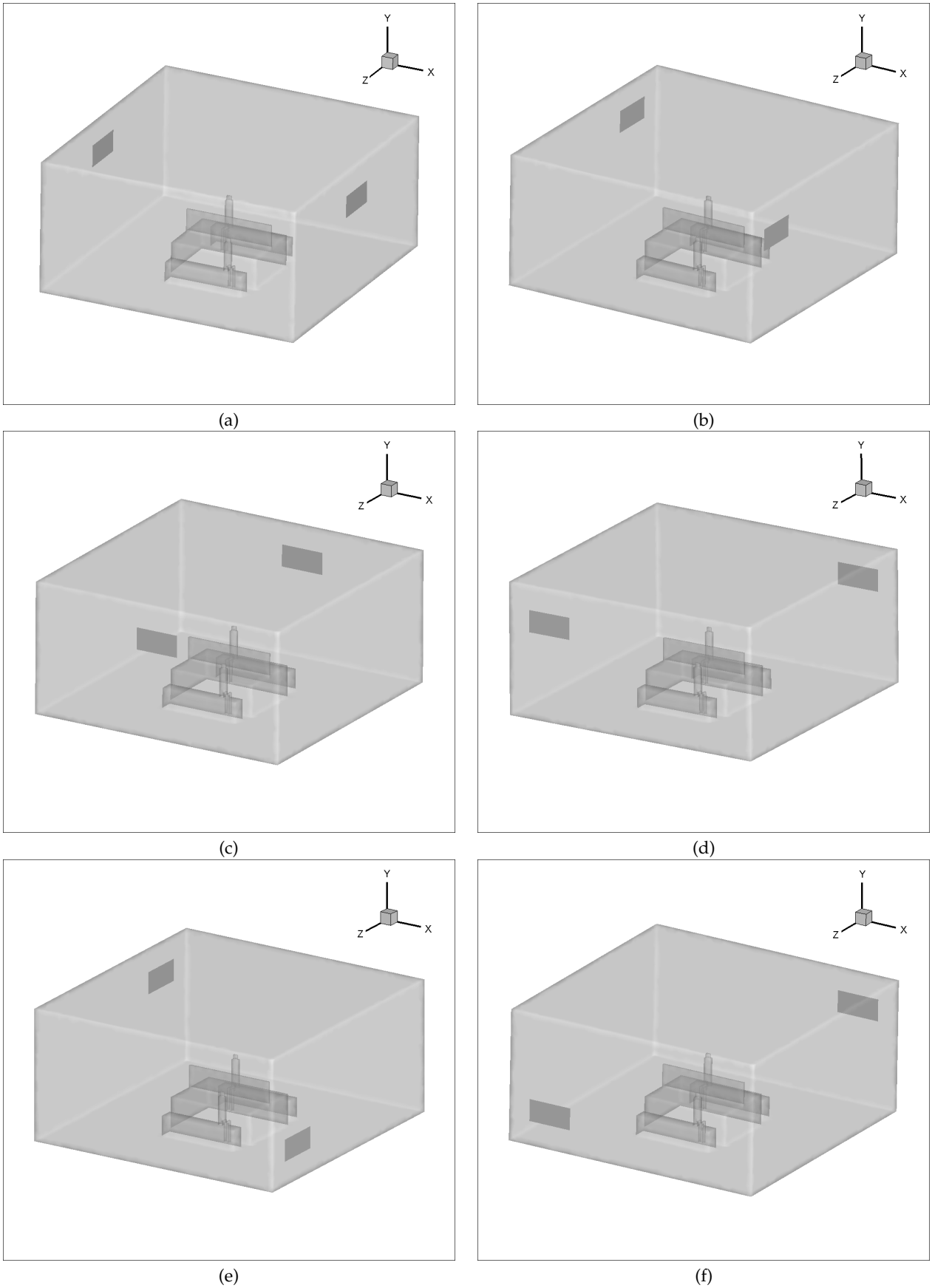

Fig. 3. Partition height of 50 cm with (a) ventilation configuration 1, (b) ventilation configuration 2, (c) ventilation configuration 3, (d) ventilation configuration 4, (e) ventilation configuration 5, and (f) ventilation configuration 6

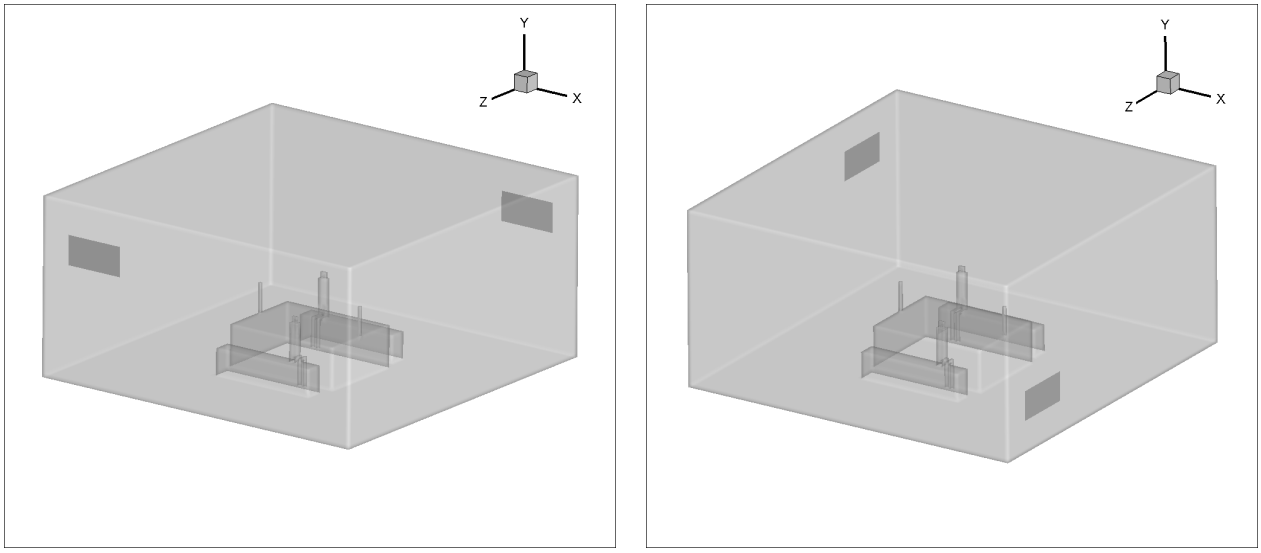

(a) (b)

Fig. 4. Air curtain height of 50 cm with (a) ventilation configuration 4, and (b) ventilation configuration 5

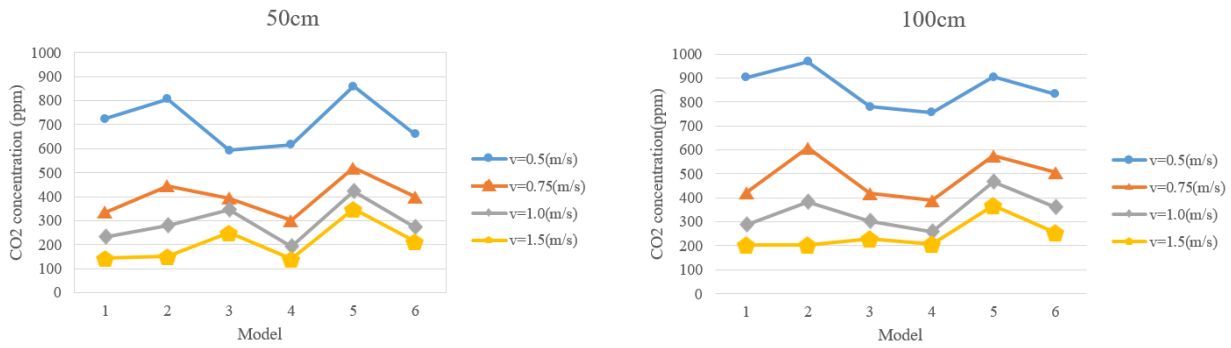

(a) (b)

Fig. 5. Carbon dioxide concentration in partition simulation with a partition height of (a) 50 cm and (b) 100 cm

1. Three-dimensional Cartesian coordinate system;
2. The fluid flow was turbulent;
3. The fluid was in a steady-state flow;
4. The fluid was not affected by gravity;
5. The walls were all no-slip walls;
6. Newtonian fluid;
7. Newtonian fluid; Partition, air curtain height: 50, 100 cm.

The numerical simulation boundary conditions are as follows:

Partition simulation:

1. Fluid: air and carbon dioxide;
2. Pollution source discharge speed was 5 m/s, carbon dioxide discharge rate was 5%, and temperature was 38°C [8–10];
3. Partition material: aluminum;
4. Air inlet: 0.5, 0.75, 1.0, 1.5 m/s, temperature was 24°C;
5. Air outlet: outflow.

Air curtain simulation:

1. Fluid: air and carbon dioxide;
2. Pollution source discharge speed was 5 m/s, the carbon dioxide discharge rate was 5%, and the temperature was 38°C;
3. Air curtain speed: 2, 4, 6 m/s;

4. Air inlet: 0.5, 0.75, 1.0, 1.5 m/s, temperature was 24°C;
5. Air outlet: outflow.

3.3. Solver setting

To analyze the accuracy of the results, double precision was set for the solver, and the numerical calculation method was SIMPLE (Semi Implicit Method for Pressure Linked Equations), serving as the theoretical basis of the calculation to perform algebraic operations and analyze turbulent flow problems. The second-order upwind scheme was adopted for kinetic energy and energy, while the first-order upwind scheme was adopted for:

1. turbulent kinetic energy 1×10^{-6};
2. k and ε residual values were 1×10^{-4};
3. continuity and velocity 1×10^{-4}.

If the above conditions were not met, the maximum number of iterations was set to 3000. The streamline distribution and concentration field of different air inlet velocities were analyzed.

4. Result and discussion

In the partition simulation, a total of 48 simulations were conducted with 4 different air inlet velocities, 6 different ventilation configurations and 2 different partition heights. Variation in ventilation configurations, air inlet velocities and partition heights will cause different effects on the concentration in the indoor space. The average carbon dioxide concentration in the indoor space under various conditions for partition heights of 50 cm and 100 cm is shown in Fig. 5(a) and Fig. 5(b), respectively. It is apparent that ventilation configuration 4 gives the best overall performance, while ventilation configuration 5 gives the worst.

In the air curtain simulation, ventilation configuration 4 and 5 were selected. A total of 48 simulations were conducted with 2 different ventilation configurations, 2 different air curtain heights, 4 different air inlet velocities, and 3 different air curtain velocities. Variation in ventilation configurations, air inlet velocities, air curtain velocities and air curtain heights will cause different effects on the concentration in the indoor space. The average carbon dioxide concentration in the indoor space under various conditions for air curtain heights of 50 cm and 100 cm is shown in Fig. 6(a), Fig. 6(b) and Fig. 6(c). It is noted that the height of the air curtain is inversely proportional to the carbon dioxide concentration in the indoor space. Increasing the air curtain height has the effect of lowering the overall carbon dioxide concentration in the indoor space and removing the virus, which results in better epidemic prevention performance and ventilation efficiency.

To investigate the concentration of carbon dioxide received by the receiver, ventilation configuration 4 was selected. When the height of the partition is relatively high, under an air inlet velocity of 0.5 m/s, the receiver receives higher carbon dioxide concentration. However, when the air inlet velocity is increased to 0.75 m/s or more, the variation in carbon dioxide concentration received by the receiver under different partition heights is insignificant. In the case with the air curtain, although the carbon dioxide concentration received by the receiver is lower when the height of the air curtain is relatively high, the overall carbon dioxide concentration received is not lower than that in the case with the partition, indicating that the effectiveness of the air curtain in terms of epidemic prevention is not as good as that of a partition as shown in Fig. 7(a), Fig. 7(b), Fig. 7(c), Fig. 7(d) and Fig. 7(e).

5. Conclusions

1. In the partition simulation, the average carbon dioxide concentration of the front-and-back ventilation configuration is lower than that of the left-and-right ventilation configuration, because the air flow direction of the front-and-back ventilation configuration is parallel to the discharge direction of the pollution source. Moreover, it is better to set the ventilation inlet/outlet near the side walls (in a diagonal fashion) rather than at the midpoint horizontally. For this reason, it can be clearly seen that the average carbon dioxide concentration in ventilation configuration 4 is lowest. When the air inlet is located at a lower position, the air flow will be blocked by the partition, making it difficult to reach the air outlet. This will in turn affect the ventilation efficiency, resulting in an increase in the concentration in the indoor space; this is evidenced by the highest average carbon dioxide concentration for ventilation configuration 5 .
2. As the air inlet velocity increases, the carbon dioxide concentration in the indoor space will decrease.
3. In the partition simulation, the higher the partition height, the higher the carbon dioxide concentration in the indoor space. As for the air curtain simulation, the result is opposite to that of the partition simulation. When the air curtain velocity reaches 4 m/s or higher, there is a lower the carbon dioxide concentration in the indoor space for a higher air curtain height.
4. From the comparison of the carbon dioxide concentra-

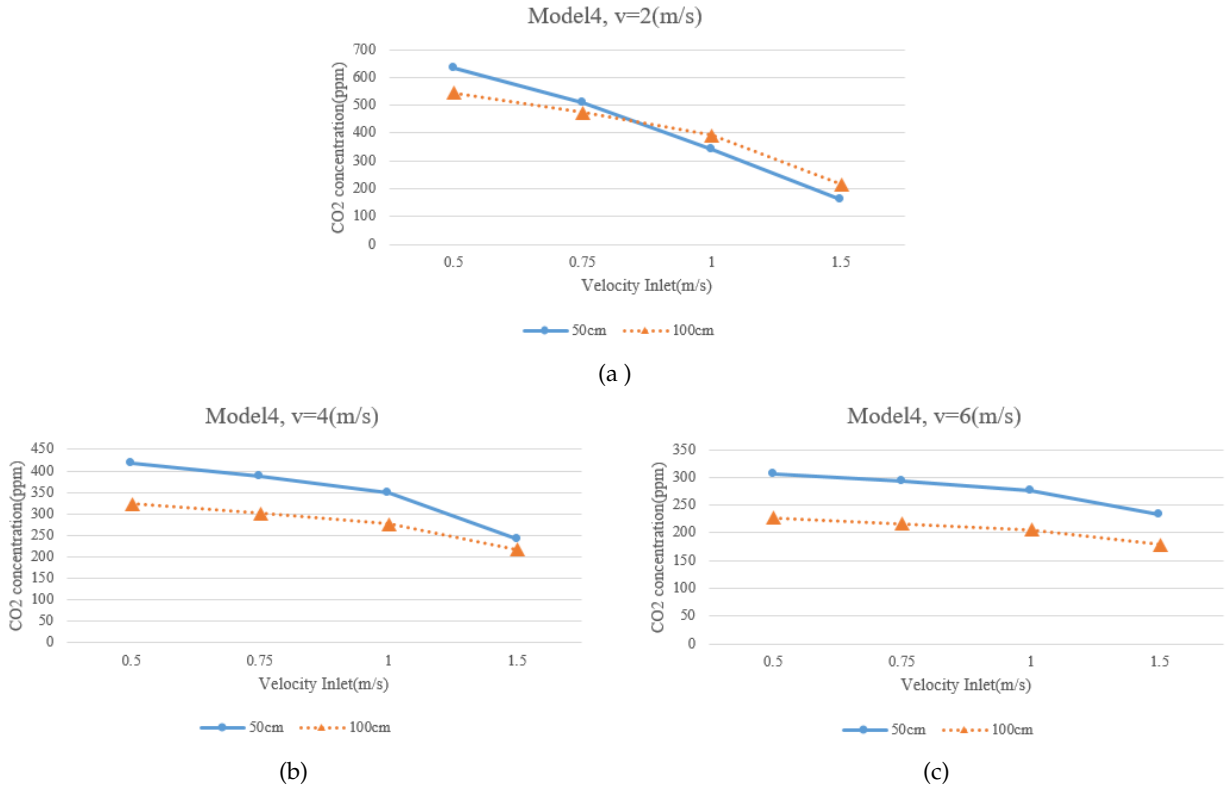

Fig. 6. Carbon dioxide concentration in air curtain simulation with ventilation configuration 4 and an air curtain velocity of (a) 2 m/s, (b) 4 m/s, and (c) 6 m/s.

Table 1. Comparison between the performance of the partition and the air curtain with ventilation configuration 4 and an air inlet velocity of 0.5 m/s

Height	Simulation type	CO_2 concentration (ppm)	Compared with partition
50 cm	Partition	616	––
	Air curtain velocity: 2(m/s)	633	-2.7%
	Air curtain velocity: 4(m/s)	417	32.3%
	Air curtain velocity: 6(m/s)	307	50.1%
100 cm	Partition	860	––
	Air curtain velocity: 2(m/s)	545	36.6%
	Air curtain velocity: 4(m/s)	323	62.4%
	Air curtain velocity: 6(m/s)	227	73.6%

Table 2. Comparison between the performance of the partition and the air curtain with ventilation configuration 5 and an air inlet velocity of 0.5 m/s

Height	Simulation type	CO_2 concentration (ppm)	Compared with partition
50 cm	Partition	756	––
	Air curtain velocity: 2(m/s)	508	32.8%
	Air curtain velocity: 4(m/s)	377	50.1%
	Air curtain velocity: 6(m/s)	287	62%
100 cm	Partition	905	––
	Air curtain velocity: 2(m/s)	457	49.56%
	Air curtain velocity: 4(m/s)	319	64.7%
	Air curtain velocity: 6(m/s)	229	74.6%

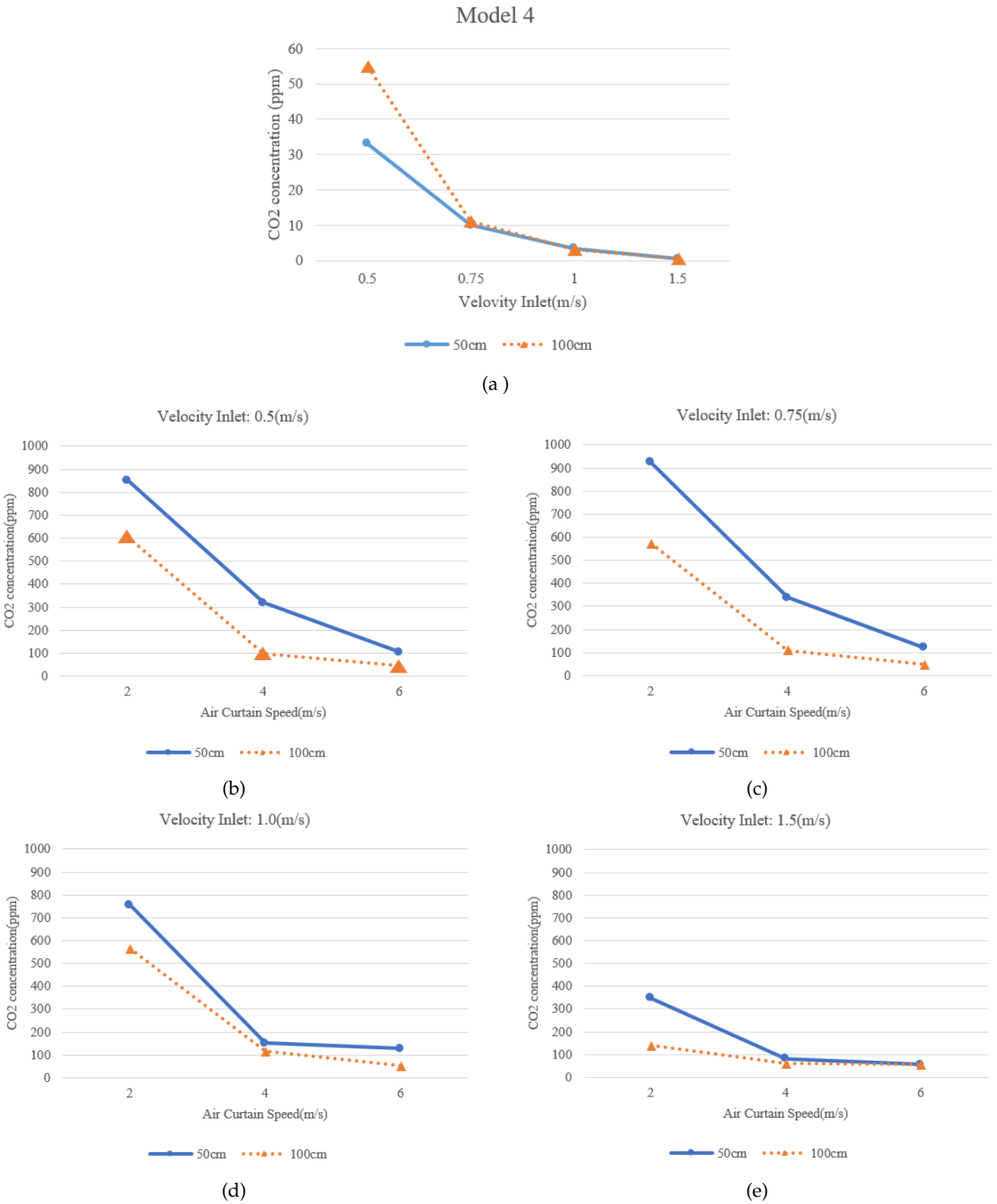

Fig. 7. (a) Comparison of the carbon dioxide concentration received by the receiver with two different partition heights, and comparison of the carbon dioxide concentration received by the receiver with two different air curtain heights under an air inlet velocity of (b) 0.5 m/s, (c) 0.75 m/s, (d) 1.0 m/s, and (e) 1.5 m/s.

tion received by the receiver, it can be seen that the concentration received by the receiver in the case of

the air curtain is higher than that in the case of the partition, suggesting that the air curtain is less effective in blocking the virus compared with the partition. Although the air curtain has the effect of improving ventilation efficiency, it is less effective in terms of epidemic prevention compared with the partition.

The results of this study show that as the height of the partition increases, although it has a higher chance of blocking the virus, it lowers the ventilation efficiency, resulting in the increase of carbon dioxide concentration in the indoor space. In the air curtain simulation, when the height of the air curtain is increased, the carbon dioxide concentration in the indoor space decreases. Although the air curtain improves the ventilation efficiency, it is less effective in terms of epidemic prevention compared with the partition. The comparison between the performance of the partition and the air curtain is shown in Table 1 and Table 2. The results show that by introducing the air curtain, the carbon dioxide concentration in the indoor space can be improved by up to 74.6% compared with the partition, indicating that the introduction of the air curtain can achieve the effect of reducing the carbon dioxide concentration.

References

[1] D. K. Chu, E. A. Akl, S. Duda, K. Solo, S. Yaacoub, H. J. Schünemann, A. El-harakeh, A. Bognanni, T. Lotfi, M. Loeb, A. Hajizadeh, A. Bak, A. Izcovich, C. A. Cuello-Garcia, C. Chen, D. J. Harris, E. Borowiack, F. Chamseddine, F. Schünemann, G. P. Morgano, G. E. U. Muti Schünemann, G. Chen, H. Zhao, I. Neumann, J. Chan, J. Khabsa, L. Hneiny, L. Harrison, M. Smith, N. Rizk, P. Giorgi Rossi, P. AbiHanna, R. Elkhoury, R. Stalteri, T. Baldeh, T. Piggott, Y. Zhang, Z. Saad, A. Khamis, and M. Reinap, (2020) *"Physical distancing, face masks, and eye protection to prevent person-to-person transmission of SARS-CoV-2 and COVID-19: a systematic review and meta-analysis"* **The Lancet *395***(10242): 1973–1987. DOI: 10.1016/S0140-6736(20)31142-9.

[2] C. Xu, X. Luo, C. Yu, and S.-J. Cao, (2020) *"The 2019-nCoV epidemic control strategies and future challenges of building healthy smart cities"* **Indoor and Built Environment *29***(5): 639–644. DOI: 10.1177/1420326X20910408.

[3] G. Cortellessa, L. Stabile, F. Arpino, D. Faleiros, W. van den Bos, L. Morawska, and G. Buonanno, (2021) *"Close proximity risk assessment for SARS-CoV-2 infection"* **Science of The Total Environment *794***: 148749. DOI: https://doi.org/10.1016/j.scitotenv.2021.148749.

[4] C. Sun and Z. Zhai, (2020) *"The efficacy of social distance and ventilation effectiveness in preventing COVID-19 transmission"* **Sustainable Cities and Society *62***: DOI: 10.1016/j.scs.2020.102390.

[5] H. S. Rahman, M. S. Aziz, R. H. Hussein, H. H. Othman, S. H. Salih Omer, E. S. Khalid, N. A. Abdulrahman, K. Amin, and R. Abdullah, (2020) *"The transmission modes and sources of COVID-19: A systematic review"* **International Journal of Surgery Open *26***: 125–136. DOI: 10.1016/j.ijso.2020.08.017.

[6] C. C. Wang, K. A. Prather, J. Sznitman, J. L. Jimenez, S. S. Lakdawala, Z. Tufekci, and L. C. Marr, (2021) *"Airborne transmission of respiratory viruses"* **Science *373***(6558): eabd9149. DOI: 10.1126/science.abd9149.

[7] C. Qin, S.-Z. Zhang, Z.-T. Li, C.-Y. Wen, and W.-Z. Lu, (2023) *"Transmission mitigation of COVID-19: Exhaled contaminants removal and energy saving in densely occupied space by impinging jet ventilation"* **Building and Environment *232***: 110066. DOI: https://doi.org/10.1016/j.buildenv.2023.110066.

[8] H. Wang, H. Qian, R. Zhou, and X. Zheng, (2020) *"A novel circulated air curtain system to confine the transmission of exhaled contaminants: A numerical and experimental investigation"* **Building Simulation *13***(6): 1425–1437. DOI: 10.1007/s12273-020-0667-5.

[9] R. Prill et al., (2000) *"Why measure carbon dioxide inside buildings"* **Published by Washington State University Extension Energy Program WSUEEP07 *3***:

[10] S. Harish, G. Nihaarikha, and R. Harish. "Computational study of Corona Virus diffusion in a closed environment". In: *IOP Conference Series: Materials Science and Engineering*. ***1128***. 1. IOP Publishing. 2021, 012004. DOI: 10.1088/1757-899x/1128/1/012004.